

As a library, NLM provides access to scientific literature. Inclusion in an NLM database does not imply endorsement of, or agreement with, the contents by NLM or the National Institutes of Health.

Learn more: [PMC Disclaimer](#) | [PMC Copyright Notice](#)

## Genes & Cancer

*Genes Cancer*. 2010 Oct;1(10):1008–1020. doi: [10.1177/1947601910395580](https://doi.org/10.1177/1947601910395580)

### Tissue Tropism of SV40 Transformation of Human Cells

Role of the Viral Regulatory Region and of Cellular Oncogenes

[Lei Zhang](#)<sup>1,2,\*</sup>, [Fang Qi](#)<sup>1,3,\*</sup>, [Giovanni Gaudino](#)<sup>1,\*</sup>, [Oriana Strianese](#)<sup>1</sup>, [Haining Yang](#)<sup>1,2</sup>, [Paul Morris](#)<sup>4</sup>, [Harvey I Pass](#)<sup>5</sup>, [Vivek R Nerurkar](#)<sup>6</sup>, [Maurizio Bocchetta](#)<sup>7</sup>, [Michele Carbone](#)<sup>1,2,✉</sup>

[Author information](#) [Article notes](#) [Copyright and License information](#)

PMCID: PMC3092263 NIHMSID: [NIHMS256443](#) PMID: [21779427](#)

#### Abstract

SV40 has been detected prevalently in a limited panel of human tumors: mesothelioma, bone and brain tumors, and lymphoma. These are the same tumor types that are specifically induced by SV40 when injected into hamsters, a finding that has raised concerns about the possible pathogenic role of SV40 in humans. Two different SV40 isolates differing in the number of 72-bp elements in the virus regulatory region, archetypal SV40 (1ESV40), which contains one 72 bp, and nonarchetypal SV40 (wtSV40), which contains two 72 bp, have been detected in human tumors. 1ESV40 has been prevalently detected in brain tumors, with wtSV40 prevalently in mesothelioma. The apparent different cell tropism could be related to the virus (i.e., possibly to the number of 72-bp elements) and to different expression of cellular genes, known to play a critical role in SV40-mediated transformation of human cells, such as Notch-1 and c-Met. To test for possible differences in tissue tropism, we infected primary human mesothelial cells (HM) and primary human astrocytes (Ast) with 1ESV40 and with wtSV40 from 2 different SV40 strains, 776 and Baylor. All viruses transformed astrocytes; only wtSV40 transformed HM. Intracellular signaling of c-Met and Notch-1 was differently induced by these 2 viruses in HM and Ast. Differences in Notch-1 expression and signaling (i.e., downstream effectors, c-Myc, HEY-1, HES-1, and HEY-L) appeared to influence SV40-mediated transformation of primary astrocytes and mesothelial cells. Our results provide a biological rationale to the observation that 1ESV40 is prevalently detected in brain tumors and wtSV40 in mesotheliomas.

**Keywords:** SV40, 72-bp elements, mesothelial cells, astrocytes, Notch-1

#### Introduction

Simian virus 40 (SV40) is a monkey virus that was isolated from polio vaccines in 1960<sup>1</sup> and later from adenovirus vaccines.<sup>2,3</sup> Soon after its identification, it was shown that SV40 was oncogenic in rodents, where it causes mesothelioma, brain and bone tumors, lymphomas, and undifferentiated sarcomas.<sup>4,5</sup> Individuals injected with SV40-contaminated vaccines developed neutralizing antibodies. Moreover, individuals that received SV40-infected vaccines, orally or via intranasal spray, excreted infectious SV40 virions several weeks after vaccination.<sup>2,3</sup> Direct contact with monkeys can also cause SV40 infection in humans.<sup>5</sup> Vertical and horizontal transmissions have been postulated as additional possible sources of infection.<sup>5</sup>

Numerous studies have looked into the serum prevalence for SV40 in the human population.<sup>5</sup> The initial discordant results were attributed to poor sensitivity in the methodologies used to reliably distinguish between SV40 and the human polyomaviruses BKV and JCV.<sup>5</sup> A reliable serological assay has been developed recently, and the authors found that 2% of a cohort of 1,501 individuals tested contained SV40-specific antibodies.<sup>6</sup>

In the SV40 regulatory region, there is a 72-bp element sequence that is unique to SV40.<sup>2</sup> SV40 isolates from polio vaccines, monkeys, and human tissues contained either one or two 72-bp elements: 1) archetypal SV40, abbreviated here as 1ESV40 (SVCPC, CPT, CPP, CPC, and Ep isolates), which contains one copy of a 72-bp element, and 2) nonarchetypal or wild-type SV40, abbreviated here as wtSV40 (SV40-776, Baylor, and VA45-54 isolates), which has two 72-bp elements.<sup>2,3</sup> The terms “nonarchetypal SV40” and “wtSV40” and “archetypal SV40” and “1ESV40” are respectively used interchangeably in this article.

SV40 DNA and proteins have been detected in about 50% of mesotheliomas, brain and bone tumors,<sup>2,5,7-9</sup> and in some types of lymphoma.<sup>10-12</sup> Notably, SV40 sequences and large T antigen (Tag) oncoprotein expression were found also in Li-Fraumeni syndrome patients, harboring heterozygous p53-inactivating mutations.<sup>13</sup> No positive correlation between SV40 sequences and mutations of p53 or Rb tumor suppressor genes was found in human osteosarcomas.<sup>14,15</sup> In most cases of SV40-positive mesotheliomas, no p53 gene mutation was detected,<sup>16</sup> in accordance with the mechanism described for SV40-mediated mesothelial cell transformation, which requires functional p53.<sup>17</sup> However, some studies have failed to identify SV40 in these tumor types or, more often, have detected SV40 only in about 5% of these tumors: these conflicting findings have led to a controversy over the possible role of SV40 in human cancer.<sup>8</sup>

Two theories have been proposed to address the discrepancies about the prevalence of SV40 in human tumor samples: according to what we will call theory 1, the geographical differences caused by the proven uneven distribution of SV40-contaminated polio vaccines around the world<sup>3</sup> and the different technical approaches used in various laboratories led to the different rates of detection.<sup>8</sup> According to what we will call theory 2, the detection of SV40 in human specimens was caused by polymerase chain reaction (PCR) contamination, when PCR was used, or by the use of nonspecific antibodies, when SV40 Tag was detected in these tumors or when ELISA assays were used, or probes, when *in situ* hybridization was used.<sup>8</sup>

Intriguingly, DNA sequencing of the virus genome detected in human tumors revealed that archetypal SV40 (1ESV40), which contains one 72-bp element in the regulatory region, was mostly detected in human brain tumors, including astrocytomas.<sup>2,5</sup> Instead, nonarchetypal SV40 (wtSV40) was most often detected in human mesothelioma.<sup>2,5</sup> Two hypotheses were formulated to address this finding, each one derived by the proponents of theory 1 or theory 2. One hypothesis is that 1ESV40 and wtSV40 have different tissue tropism. The differences in tissue tropism could be related to the infectious virus or to the cell type or to both. If this hypothesis was correct, it would support “theory 1,” that is, see above. The second hypothesis comes from the proponents of theory 2 and proposes that because different laboratories are contaminated with different SV40 isolates, they will detect one or two 72-bp elements in whatever set of samples they are analyzing: in other words, that the “specific” association is in fact caused by “specific” PCR contamination. Because plasmids containing SV40 sequences have been used in many laboratories, there is a rationale to support this theory.<sup>8</sup>

Here, we present a set of experiments that were designed to investigate the possible biological reasons that might cause a specific viral tissue tropism. Our results address these 2 opposing theories. Below is a summary of general background information necessary to understand the design of these experiments.

Tag and the small t antigen (tag) are the 2 SV40 oncogenes.<sup>2,5</sup> When their coding sequences are under the control of a heterologous promoter, a wide range of cells can be transformed, virtually any cell type.<sup>2,5</sup> This is in sharp contrast with the observation that most human cell types are lysed and only rarely become transformed following SV40 infection, with the notable exception of HM that are susceptible to SV40 transformation.<sup>2,5</sup> Our hypothesis was that tissue tropism might be triggered by the virus regulatory regions. Alternatively or in addition, cell type-specific differences in the expression levels of some host protein(s) that are known to play a key role in SV40 oncogenesis,<sup>5</sup> such as Notch-1<sup>18</sup> and c-Met,<sup>19</sup> might influence tissue tropism. To test this hypothesis, we infected primary HM and primary Ast with 2 different strains of SV40 (776 and Baylor), carrying either one or two 72-bp elements. In both strains, the viruses differ only by the duplication of the element, while they share the remaining sequences, including the Tag carboxyl-terminal end. We studied the outcomes of the infection and the expression of c-Met and Notch-1 and downstream effectors in these cells.

Our results reveal that all viruses transformed Ast, while HM were transformed only by viruses carrying 2 enhancer elements, either 776 or Baylor strains. Intracellular signaling of c-Met and Notch-1 was higher in nonarchetypal SV40 than in 1ESV40-infected HM. The biological effects of viral infection were influenced by the number of 72-bp repeats present (archetypal v. nonarchetypal configuration) and were not influenced by the viral strain (776 v. Baylor). Our results provide a biological rationale for the finding that 1ESV40 is prevalently detected in brain tumors and nonarchetypal SV40 in mesotheliomas.

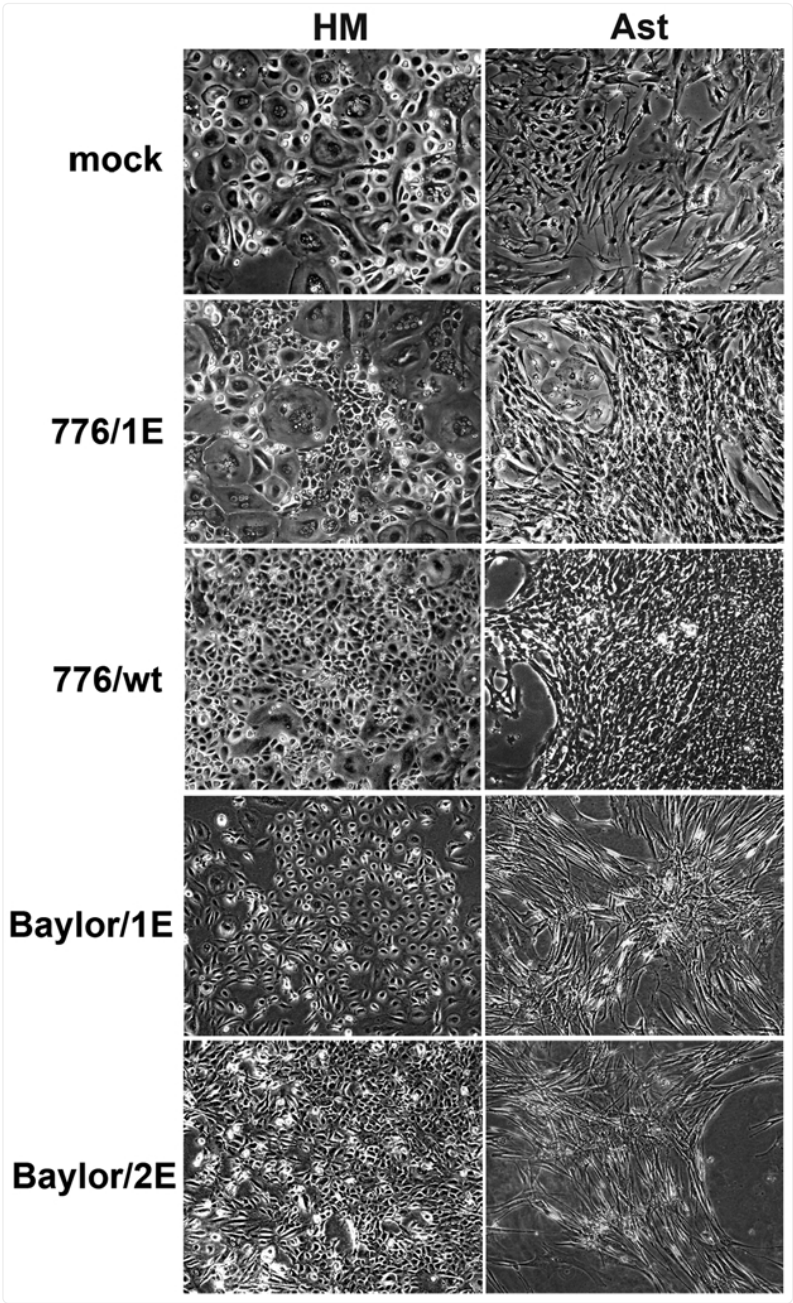
## Results

### Astrocytes and mesothelial cells are differently susceptible to wtSV40 and 1ESV40

To compare the infectivity of archetypal and nonarchetypal SV40, primary HM and primary Ast were seeded on chamber slides and infected with equal amounts of 2 different SV40 virus strains (776 and Baylor). Both viruses carried either 1 copy of the enhancer element (1ESV40: 776/1E, Baylor/1E) or 2 copies of the enhancer element (wtSV40: 776/wt, Baylor/2E). The virus titer was determined on permissive CV1 monkey cells as previously described.<sup>20</sup> Three days postinfection, a percentage ranging from 40% to 80% of SV40 Tag-positive cells was detected in HM and Ast infected with 1ESV40 and wtSV40 at multiplicity of infection (MOI) of 10 plaque-forming units (PFU) per cell (Suppl. Fig. S1A). No differences were observed in the number of Tag-positive cells in HM and Ast cultures when infected with wtSV40 or with 1ESV40 (Suppl. Fig. S1B). Cells infected with 1ESV40 and wtSV40 displayed a comparable amount of SV40 DNA, as determined by real-time PCR, 24 hours postinfection (data not shown). These results indicate that the 2 viruses (1ESV40 and wtSV40) have equal ability to infect HM and Ast.

Upon SV40 infection at MOI of 10, both HM and Ast underwent morphological changes (Fig. 1), and “flat foci” developed 2 weeks postinfection. These “flat foci” were collected with a pipette tip and propagated in culture. SV40-mediated transformation is mainly a function of Tag.<sup>2</sup> Thus, we tested whether different amounts of Tag mRNA and protein were produced in early stages (72 hours postinfection) of infection in HM and in Ast. The levels of expression of Tag, determined by quantitative reverse transcription polymerase chain reaction (qRT-PCR) and by Western blotting, were higher in early infections with both strains of nonarchetypal SV40 than in those infected with 1ESV40 (Fig. 2A and 2B). We anticipated that the higher levels of Tag detected in nonarchetypal SV40 infections would correlate with a higher efficiency of cellular transformation compared to 1ESV40 infections.

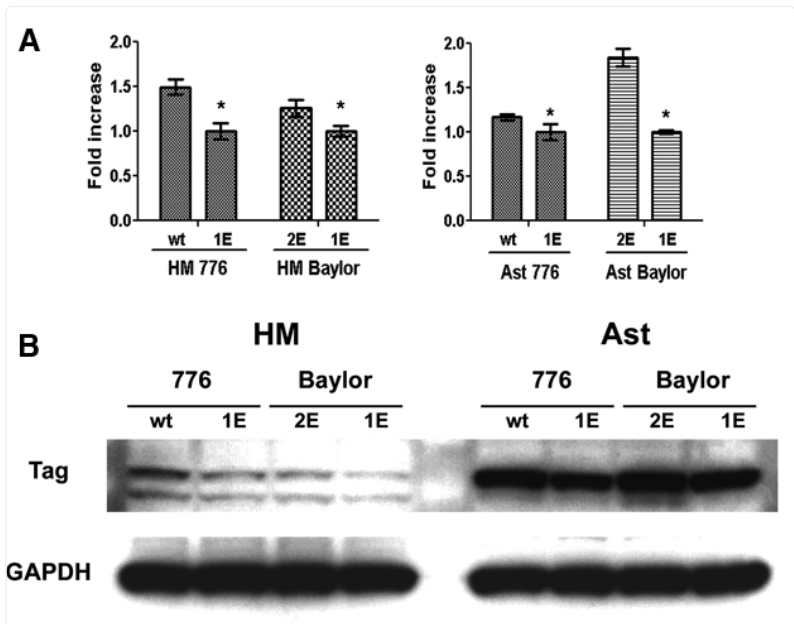
Figure 1.



[Open in a new tab](#)

SV40 infection induces changes in the morphology of HM and Ast. Both wtSV40 and 1ESV40 caused “morphological transformation” of HM and Ast in tissue culture (i.e., upon infection, the cells become spindle and refrangent and form “flat foci,” where cells are particularly dense without forming a tridimensional piling-up focus). “Flat foci” were rare in flasks containing HM infected with 1ESV40. Original magnifications, 40x.

Figure 2.



[Open in a new tab](#)

Seventy-two hours postinfection, Tag is highly expressed in wtSV40-infected HM and Ast. The levels of Tag in HM and Ast infected by wtSV40 of both 776 and Baylor strains are higher than in 1ESV40-infected cells. (A) qRT-PCR of Tag in cells 72 hours postinfection with the different viruses. Asterisks indicate significant differences between the amount of Tag mRNA expressed by different cells, as indicated. (B) Western blots showing amounts of Tag protein produced 72 hours postinfection with wtSV40 or 1ESV40 in both HM and Ast.

Strikingly, only HM infected by nonarchetypal SV40 (776/wt, Baylor/2E) formed colonies in soft agar; HM infected by 1ESV40 (776/1E, Baylor/1E) did not (Table 1). Instead, Ast infected by either 1ESV40 and nonarchetypal SV40, irrespective of the strain used, formed colonies in soft agar. Colony formation in soft agar is regarded as a measure of *in vitro* malignant transformation<sup>21</sup>; thus, 1ESV40 was able to cause malignant transformation of Ast but not of HM, a finding that appeared to support the observation that 1ESV40 was detected prevalently in brain tumors and not in mesotheliomas. Ast transformed by 776/wt or Baylor/2E formed significantly more colonies than those transformed by 776/1E or Baylor/2E ( $P = 0.03$  or  $P \leq 0.0001$ , respectively), and Ast transformed by 776/1E or Baylor/1E formed significantly more colonies than HM transformed by 776/wt or Baylor/2E ( $P = 0.007$  or  $P = 0.0003$ , respectively) (Table 1).

Table 1.

SV40-Induced Transformation in Human Cells

Infected Cells	Colonies × 10 <sup>4</sup> Cells in Soft Agar (n = 5)
HM 776/1E	0
HM Baylor/1E	0
HM 776/wt	9 ± 5
HM Baylor/2E	4 ± 1
Ast 776/1E	545 ± 62
Ast Baylor/1E	271 ± 72
Ast 776/wt	1,400 ± 132
Ast Baylor/2E	1,152 ± 88

[Open in a new tab](#)

Note: Growth in soft agar: 1 × 10<sup>4</sup> cells from cultures propagated from foci, after cell infection with the different viruses, were seeded on 0.3% to 0.6% agar in DMEM 10% FBS. Statistical significance: Ast 776/wt versus Ast 776/1E (*P* = 0.03); Ast Baylor/2E versus Ast Baylor/1E (*P* ≤ 0.0001); Ast 776/wt versus HM 776/wt (*P* = 0.007); and Ast Baylor/2E versus HM Baylor/2E (*P* = 0.0003). 1ESV40 cause transformation of Ast but not HM. Soft agar growth of cell infected by different viruses and viral strains. This experiment has been repeated 5 times on each of 2 primary HM and Ast from separate donors.

Together, these results revealed that Ast are much more susceptible to SV40-mediated transformation than HM. Possibly, the higher levels of Tag expression induced by nonarchetypal SV40 infection are required to transform HM, while the lower levels of Tag mRNA and protein, produced by 1ESV40 infection, are sufficient to transform Ast.

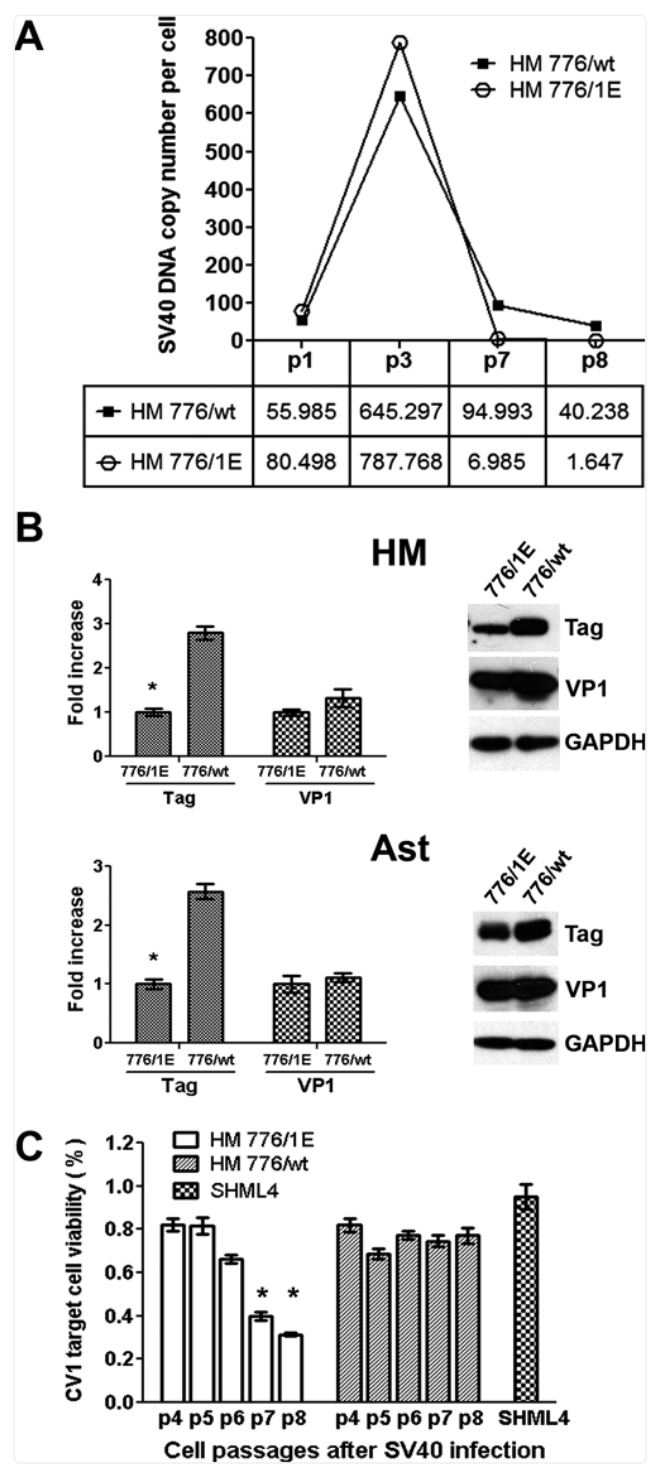
Higher amounts of Tag in wtSV40-infected cells are linked to transcription/translation regulation rather than DNA amplification

Infectious SV40 particles have been rescued from patient biopsies, suggesting that the virus is not integrated in the tumor cell genome or at least that some of the virus remains episomal.<sup>8</sup> This finding is in accordance with the observation that SV40 remains largely episomal in human mesothelial cells infected in tissue culture.<sup>22,23</sup> In the experiments described here, HM and Ast contained episomal SV40 and showed no detectable viral integration in early tissue culture passages (Suppl. Fig. S2). However, integration of SV40 was observed after passage 10 (data not shown). This finding supports a role for the episomal virus in initiating and maintaining cellular transformation, at least during early passages in tissue culture.

We compared the SV40 viral load in HM 776/1E (HM infected with 1ESV40) and in HM 776/wt (HM infected with wtSV40) by quantification of SV40 DNA copy number using real-time PCR. Serial dilutions of SV40 plasmid were used as a standard curve, and DNA loading was normalized using GAPDH DNA copy number. The copy number profile along with the different passages revealed a decrease of viral load after a peak of virus replication, both in HM 776/1E and in HM 776/wt as they were propagated in tissue culture. The results showed that HM infected by either 1ESV40 or wtSV40 had similar amounts of viral loads and kinetics (Fig. 3A). Comparable amounts in SV40 copy numbers and a similar profile of viral replication were also observed in 1ESV40-infected Ast (Ast/1E) and non- archetypal SV40-infected Ast (Ast/wt) (data not shown).



Figure 3.



[Open in a new tab](#)

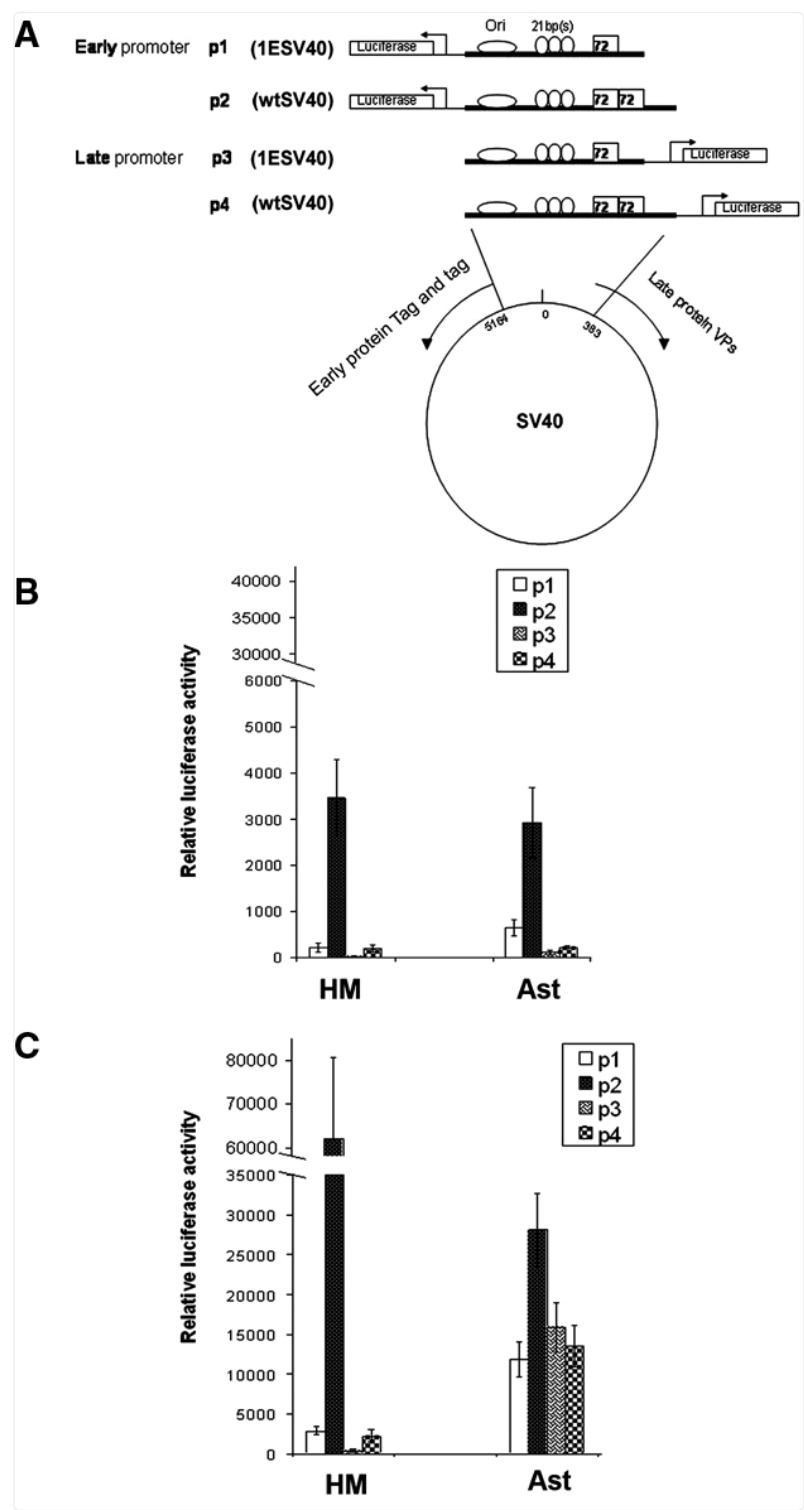
SV40 DNA copy numbers, viral particle release, and early/late gene expression in cells infected with wtSV40 and 1ESV40. (A) SV40 DNA copy number. Real-time PCR of SV40 DNA present in infected cells at different passages postinfection, using a serial dilution of SV40 plasmid as a standard curve. DNA loading was normalized by GAPDH. Based on the notion that 1 ng of genomic DNA =  $1.5 \times 10^3$  cells, we calculated the approximate SV40 DNA copy number per single cell. The results for HM/1E and HM/wt are reported here, and comparable results were obtained for Ast/1E and Ast/wt (data not shown). Tissue culture passage numbers are p1, p3, p7, and p8. Cells were split every 3 days. (B) Levels of Tag and VP1 mRNA (left panel) and protein (right panel) in HM and Ast infected with wtSV40 and 1ESV40 (passage 3). Tag levels were higher in HM and Ast infected with wtSV40 compared to 1ESV40-infected cells. VP1 transcripts and proteins did not show detectable differences. (C) Virus release. CV-1-permissive cells were incubated with the conditioned medium of cultures at passages 4 to 8 after infection, when transformation may occur, and cell viability was evaluated by MTT to assess the release of viral particles. SHML4: SV40-transformed HM established a cell line (over a hundred passages), where virus release is barely detectable. This experiment was repeated 3 times (each time,  $n = 4$ ). Bars: standard deviation. Asterisks indicate significant difference compared to passage 4 ( $P \leq 0.0001$ ).

To verify the production of SV40-infectious viral particles, we exposed monkey CV-1 cells, susceptible to SV40-productive infection, to the supernatants collected from HM- and Ast-infected cells at passage 4 and, thereafter, soon after the peak of viral DNA production occurred in infected cells ([Fig. 3A](#)). Compared to Tag levels detected 72 hours postinfection (i.e., before cells become transformed), non-archetypal SV40-infected HM (HM/wt) and Ast/wt showed higher expression levels of Tag mRNA and protein compared to 1ESV40-infected HM (HM/1E) and Ast/1E. VP1 late gene transcripts and protein expression did not show significant differences among cells infected with 1ESV40 and nonarchetypal SV40 ([Fig. 3B](#)). These results suggested that the 72-bp elements influenced transcriptional regulation. The conditioned medium of an established transformed mesothelial cell line (SHML4, passed in tissue culture more than 100 times) was tested as well. Ast/wt and HM/wt and Ast/1E released a constant amount of viruses along all passages (i.e., as measured by CV-1-induced cell lysis). Instead, the cytotoxicity induced by HM 776/1E-conditioned media increased during passage in tissue culture ([Fig. 3C](#)). These data correlated with the observation that 1ESV40 did not induce HM transformation ([Table 1](#)). Only a very limited cell lysis was induced by supernatants derived from SHML4 (i.e., rare, about 1% of cells developed the classic SV40-induced vacuoles, indicative of productive infection that leads to cell lysis) (data not shown) ([Fig. 3C](#)).

### The 72-bp elements enhance transcription of SV40 early genes

To verify the possible impact of the different number of the 72-bp sequence on the transcriptional activity of 1ESV40 and wtSV40, 4 gene reporter constructs were prepared. The firefly luciferase gene was positioned under the control of the 2 SV40 regulatory regions, containing one or two 72-bp elements, in 2 opposite directions. The 4 resulting plasmids mimicked the early gene promoters (p1 and p2) or the late gene promoters (p3 and p4), driving the expression of Tag and tag early proteins and of VPs capsid proteins, respectively ([Fig. 4A](#)). The sequence of the regulatory regions was from the SV40 776 strain,<sup>2,3,23</sup> starting immediately upstream of the ATG codon for early proteins and encompassing the first intron of the VPs capsid proteins gene. The intron was included because of its role in transcriptionally regulating late protein expression.<sup>2,24</sup> Reporter plasmids were transfected in HM and Ast, and luciferase activity was measured 36 and 48 hours posttransfection. The luminescent signals were normalized to the copy number of transfected plasmids, determined by the internal standard Renilla luciferase reporter, as described in Materials and Methods.

Figure 4.



[Open in a new tab](#)

Reporter assay demonstrating the enhancer effect of 72-bp elements and autoregulation of SV40 early protein on its early transcripts. **(A)** Schematic illustration of the 4 reporter constructs (plasmids): p1 and p2 contain the early promoter; and p3 and p4 contain the late promoter. **(B)** Basal luciferase activity of the different constructs upon infection of primary human HM and Ast. **(C)** Cotransfection of the pEarly plasmid<sup>13</sup> with the reporter constructs strongly activating early promoters in HM and Ast cells (compare the results to **B**). Results were reproducible in 2 separate primary HM and Ast. In all reporter assays, the y-axis values are normalized by luciferase gene copy number, according to the ratio of the luciferase activity of firefly versus that of Renilla internal standard. Each value is subtracted by the background signal from cells transfected with the promoterless control pGL4.10.

The nonarchetypal SV40 constructs p2 and p4 (Fig. 4A), with two 72-bp elements, enhanced the transcription of early and late promoters, respectively, in both cell types, as compared to the 1ESV40 p1 and p3 plasmids, carrying only one 72-bp sequence. Notably, the ratio between early promoter activities (p1/p2) was similar in HM and Ast (Fig. 4B). These results suggest that the 72-bp consensus sequence acts as an amplifier of the transcriptional enhancer activity.



SV40 Tag protein binds cooperatively to 3 tandem sites at the regulatory region of SV40 DNA.<sup>2,24</sup> We verified the Tag regulatory activity by cotransfecting the reporter plasmids described above ([Fig. 4A](#)) with the pEarly plasmid, which constitutively express Tag.<sup>18</sup> Luciferase activity was measured as described above. The constitutive expression of recombinant Tag led to a further and relevant increase of promoter activity of the early constructs p1 and p2 in both HM and Ast cells but not of the late constructs p3 and p4 ([Fig. 4C](#)). These results reveal that, also in the presence of high levels of Tag, the 72-bp element retains the function of transcription amplifier for the early promoters, which are the promoters associated with the virus-transforming activity. This evidence of the enhancer function for the 72-bp element is reminiscent of previous findings.<sup>25</sup>

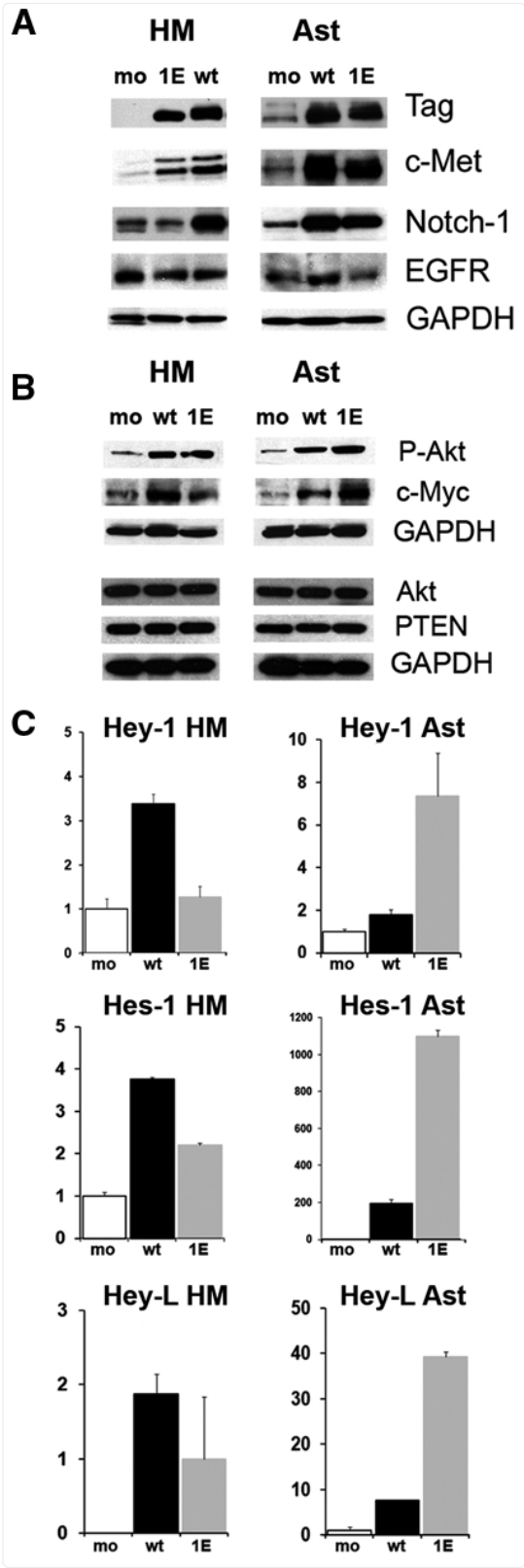
### Differential targeting of Met and Notch1 in infected cells

1ESV40 and nonarchetypal SV40 induced malignant transformation of Ast in soft agar; instead, only HM/1E did not grow in soft agar. We hypothesized that Ast might have some biological feature that makes them more susceptible to SV40-mediated transformation.

To address this hypothesis, we examined the expression and signaling of c-Met (hepatocyte growth factor receptor) and Notch-1 in HM and Ast. These receptors are specifically activated by SV40 infection and contribute to SV40-mediated malignant transformation.<sup>18,19,26</sup>

Nonarchetypal SV40 infection of HM and Ast induced an increase of c-Met and Notch-1 expression. 1ESV40 infection of Ast induced similar changes in c-Met and Notch-1 expression ([Fig. 5A](#)). Instead, in HM/1E, Notch-1 was not induced, and only a slight increase in c-Met expression was observed ([Fig. 5A](#)). Notably, the levels of c-Met and Notch-1 seem specifically targeted by SV40, since the expression of another tyrosine kinase receptor in HM and Ast, the epidermal growth factor receptor (EGFR), was not influenced ([Fig. 5A](#)). We found that the Akt-1 kinase, a downstream effector of c-Met, was phosphorylated (activated) in SV40-infected cells ([Fig. 5B](#)). The Akt protein levels were not influenced by SV40 infection, indicating that the increased kinase activity was not due to transcriptional regulation. Phosphatase and tensin homolog (PTEN) expression, a known regulator of the PI3K/Akt/mTOR axis, was not influenced by SV40 infection ([Fig. 5B](#)), suggesting that, in SV40-infected human cells, c-Met was the main regulator of Akt.

Figure 5.



[Open in a new tab](#)

SV40 infection induction of c-Met and Notch-1 is cell type and viral type dependent. (A) Immunoblotting analysis for SV40 Tag, c-Met, and Notch-1 in transformed HM (left) and Ast (right), 72 hours after infection. Infection with either viruses leads to induction of c-Met and Notch-1; EGFR was not influenced. Please note the different position of lanes “1E” and “wt” in HM (left) and Ast (right) blots. (B) Immunoblotting analysis of p-Akt (i.e., Akt activity) and of total protein expression for Akt-1 (c-Met downstream pathway) and PTEN (Akt regulator) and total protein expression of c-Myc (Notch-1 downstream pathway). SV40 induced Akt-1 activity and c-Myc expression; PTEN is unaltered. GAPDH was used as loading control. (A and B) mo = mock-infected cells; wt = wtSV40-infected cells; 1E = 1ESV40-infected cells. (C) qRT-PCR analysis of Hey1, Hes1, and HeyL, the major Notch-1 signal

transduction effectors in HM and Ast. White bars = uninfected cells; black bars = cells infected with wt SV40; light gray bars = cells infected with 1ESV40. Note the different cell type-dependent effects on Notch-1 expression caused by infection with wtSV40 and 1ESV40.

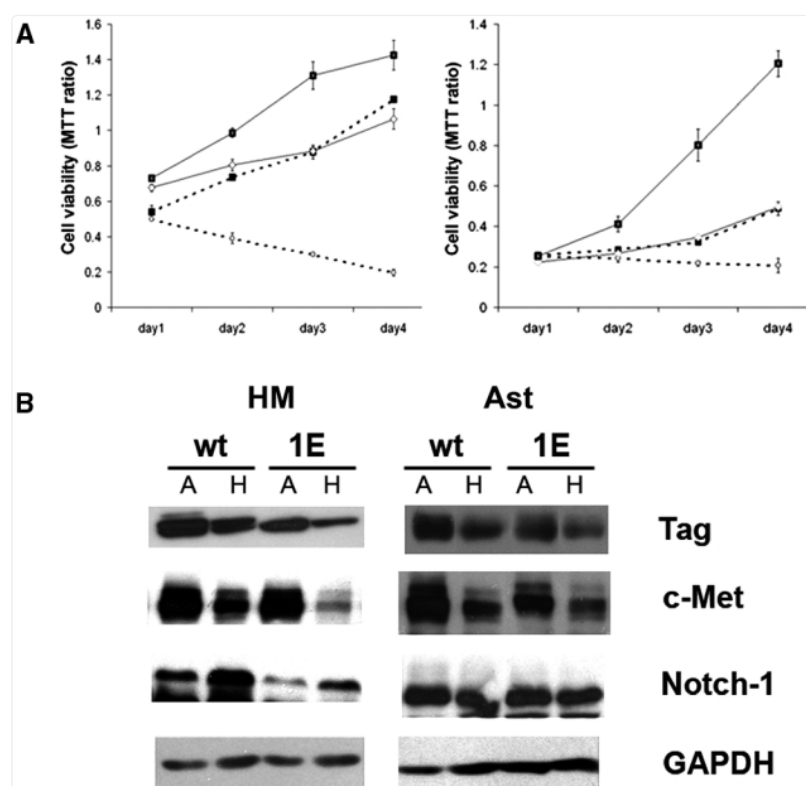
The expression of the Notch-1 transcriptional target c-Myc was notably higher in HM/wt compared to HM/1E. Instead, in Ast, 1ESV40 infection induced higher amounts of c-Myc protein than wtSV40 ([Fig. 5B](#)). We verified this unexpected finding by testing the expression of additional downstream Notch-1 targets, HEY-1, HES-1, and HEYL-1. Quantitative real-time PCR revealed that the basal level of Notch-1 signaling was higher in HM than in Ast. In Ast, 1ESV40 induced HEY-1, HES-1, and HEYL-1 more efficiently than wt/SV40. Instead, in HM, HEY-1, HES-1, and HEYL-1 were induced more efficiently by wtSV40 ([Fig. 5C](#)). These findings matched the different changes observed in the expression of c-Myc upon infection with the 2 viruses. Together, these results uncovered cell type-specific responses of Notch-1 signaling in response to infection with nonarchetypal and 1ESV40 ([Fig. 5C](#)). Nonarchetypal SV40 induced Notch-1 signaling more efficiently in HM compared to Ast; in contrast, 1ESV40 induced Notch-1 in Ast but not in HM.

We have previously shown that Notch-1 activation is a critical requirement for wtSV40-mediated transformation of HM.<sup>18</sup> Thus, we tested the hypothesis that the inability of 1ESV40 to induce Notch-1 in HM was related to the inability of 1ESV40 to transform these cells.

### Notch-1 determines the survival of cells grown in suspension

We tested whether Notch-1 expression was required for anchorage-independent growth (a test used to measure transformation in tissue culture) of SV40-infected HM and Ast. To test this hypothesis, we grew cells in suspension by plating them on an anti-adhesive polymer poly (2-hydroxyethyl methacrylate [polyHEMA])-coated plates. Primary HM and Ast cells did not grow on polyHEMA plates, as shown by the MTT assay (data not shown). HM/wt and Ast/wt grew on polyHEMA. HM/1E did not grow on polyHEMA, and the MTT assay showed a marked decrease in cell viability. Ast/1E showed some moderate growth on polyHEMA ([Fig. 6A](#)). Immunoblotting analysis was performed on HM and Ast 72 hours after SV40 infection, in the different growing conditions. Compared to cells grown "attached" (A), HM and Ast in polyHema (H) had lower amounts of Tag and c-Met. Instead, Notch-1 expression was increased in HM/wt and in HM/1E grown in polyHema. The high levels of Notch-1 detected in SV40-infected Ast were not influenced by the type of growth ([Fig. 6B](#)).

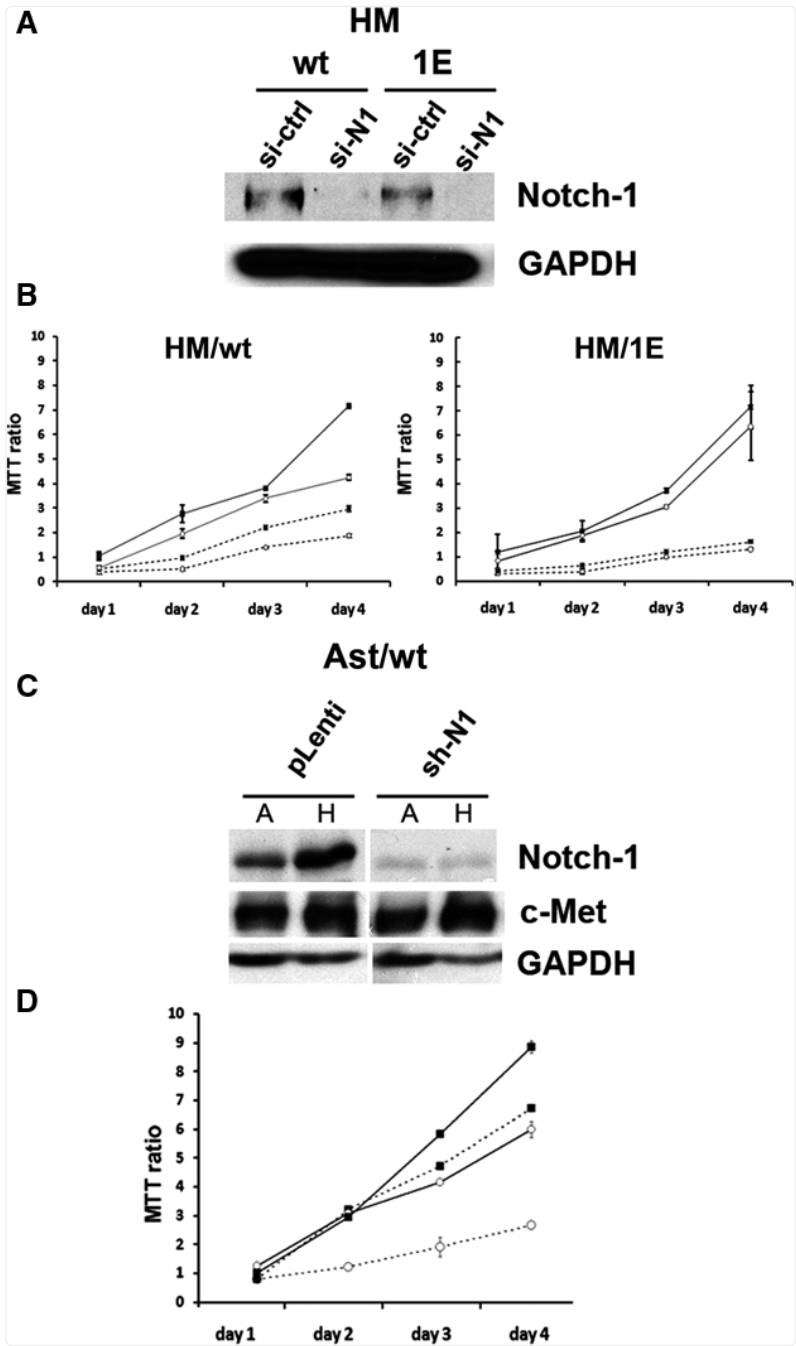
Figure 6.


[Open in a new tab](#)

Growth curves and oncogene expression of HM and Ast when grown attached or in suspension. (A) HM (left panel) and Ast (right panel). HM/1E showed a decrease of the MTT reading in polyHEMA-coated plates. HM/wt, Ast/wt, and Ast/1E showed sustained or increased MTT values when grown in polyHEMA. Seventy-two hours after infection, HM (left) were seeded at a density of  $4 \times 10^3$ /well in a 96-well plate, and Ast (right) were seeded at a density of  $1.5 \times 10^3$ /well to accommodate the fast growing Ast/wt. On day 1, the y-axis values of HM/1E-hema and Ast/1E-hema were denoted as 1; the y-axis values on the following days represent the ratio of the MTT readout relative to day 1. Experiments were performed in triplicate. Solid lines (—) = attached growth; dotted lines (- - -) = growth on polyHema; black square (■) = cells infected with wtSV40; white circle (○) = cells infected with 1ESV40. (B) Immunoblotting analysis performed on day 2 in cells grown in polyHEMA (H) or attached (A). Note the decrease in Tag and c-Met expression in cells grown in polyHEMA. HM show an increase in Notch-1 expression in cells grown in polyHEMA.

We tested the hypothesis that the acquired capability of SV40-infected HM and Ast to grow in suspension was related to the expression of Notch-1. We performed gene silencing experiments by transfecting HM/wt and HM/1E with siRNA oligonucleotides specifically targeting Notch-1 (see Materials and Methods). Western blotting showed that Notch-1 expression was specifically and markedly reduced 48 hours after transfection, with siRNAs targeting Notch-1 mRNA (Fig. 7A). The viability of HM silenced for Notch-1 expression was evaluated by the MTT assay, in both attached and polyHEMA growth conditions. The growth of HM/wt in attached conditions was not reduced by Notch-1 silencing during the first 72 hours after transfection; thereafter, the growth curve started to decrease. When grown in polyHEMA (cells in suspension), silencing of Notch-1 reduced the ability of HM/wt-infected cells to grow from day 1. Notch-1 silencing in HM/1E did not influence cell growth regardless of the growth conditions (Fig. 7B), a finding that was in accordance with the negligible Notch-1 expression in HM upon 1ESV40 infection (Fig. 5A).

Figure 7.



[Open in a new tab](#)

Role of Notch-1 in SV40-mediated transformation of HM and Ast. (A) Notch-1 silencing in HM infected with wtSV40 and 1ESV40. Western blotting was performed 48 hours after transfection with Notch-1 siRNA (si-N1) or with “scramble” control oligonucleotide (si-ctrl). Note the reduction of Notch-1 expression in cells transfected with si-N1. GAPDH was used as the loading control. (B) Cell viability was measured by the MTT assay in triplicate. HM, 72 hours after infection with 1ESV40 and wtSV40, were analyzed 24, 48, 72, and 96 hours after transfection with siRNA oligonucleotides. Solid lines (—) = attached growth; dotted lines (---) = growth on polyHema; black square (■) = cells transfected with “scramble” control siRNA; white circle (○) = cells transfected with Notch-1 siRNA. (C) Immunoblotting analysis performed on day 7 after lentivirus transduction, in cells grown in polyHEMA (H) or attached (A). Specific knockdown of Notch-1 in Ast/wt cells is shown, as c-Met expression (control) is not affected. (D) Cell viability (MTT) assay was done in triplicate, as in B, upon Notch-1 knockdown. Ast/wt cells showed decrease of anchorage-independent growth and proliferation. Solid lines (—) = attached growth; dotted lines (---) = growth on polyHema; black square (■) = cells transduced by control p-Lenti vector; white circle (○) = cells transduced with Notch-1 shRNA.

When using siRNAs, we could not significantly reduce Notch-1 in nonarchetypal SV40- and in 1ESV40-infected Ast (data not shown), a result that we attributed to the high levels of Notch-1 expression in these cells (Fig. 6B). Therefore, Notch-1 knockdown was performed in Ast/wt using shRNA delivered by lentivirus, as described in Materials and Methods. When using the lentiviral system, we were able to reduce Notch-1 expression to levels equivalent to the reduction observed when using siRNA in HM (Fig. 7C). Using the MTT assay, we measured cell viability in Notch-1-silenced Ast growing attached, and we detected a marked

reduction in cell viability, starting 48 hours after silencing. In Ast grown in polyHEMA, Notch-1 knockdown markedly impaired their ability to grow, indicating that the growth of these cells is dependent on SV40-induced Notch-1 expression ([Fig. 7D](#)). Similar results were obtained with Ast/1E cells after Notch-1 knockdown (data not shown). This is in accordance with the comparable levels of Notch-1 induced by wtSV40 and 1ESV40 in Ast. These results demonstrate the role of Notch-1 in promoting cell survival, especially when cells are grown in suspension and provide a possible explanation of the unusual susceptibility of Ast to SV40 transformation.

## Discussion

Different SV40 strains, 776 and Baylor strains, produced very similar results upon infection of human HM and Ast: instead, the number of 72-bp elements present in the enhancer region (archetypal v. nonarchetypal configuration) influenced the outcome of these infections. Specifically, we found that the wtSV40 (nonarchetypal) is much more potent than 1ESV40 (archetypal) in causing malignant transformation of HM *in vitro*. In Ast, this difference is less pronounced and appears related to the very high susceptibility of these cells to SV40 transformation. Actually, the susceptibility of Ast uncovered by our experiments ([Table 1](#)) is remarkable, considering that so far, mesothelial cells were considered the cell type most susceptible to SV40-mediated transformation.<sup>5</sup>

Our results provide an experimental rationale to the observation that archetypal SV40 is often found in brain tumor biopsies and nonarchetypal SV40 is found more often in mesotheliomas. Archetypal SV40 is a much more common virus than nonarchetypal SV40. For instance, the vast majority of SV40 isolates from SV40-infected polio and adeno vaccines were archetypal SV40.<sup>2,3</sup> SV40-contaminated vaccines were distributed until 1963 in the United States and in most parts of the world.<sup>2,3</sup> However, USSR polio vaccines, used in every country that was under the influence of the USSR, contained infectious SV40 until at least 1978.<sup>3</sup> In Italy, until 1999, at least one seed from which polio vaccines were manufactured was contaminated with SV40. While none of the 4 vaccine lots tested were contaminated and no live virus was recovered from the seed, when the Italian authorities were informed of this fact, production of the vaccines switched to the World Health Organization (WHO) polio seed (Phil Minor, personal communication, March 2010).<sup>27</sup> Some countries such as China still produce polio vaccines in monkey tissues, and such vaccines may contain SV40.<sup>3</sup> In other words, human exposure to SV40 through contaminated polio vaccines has been vast and has been influenced by geographical differences associated with the use of contaminated or noncontaminated vaccines. Therefore, humans have been exposed to multiple strains of SV40; most of these were archetypal strains with one 72 bp in the enhancer region (by far, the most common strain present in polio vaccines<sup>2,3</sup>); some were nonarchetypal (i.e., also known as wild-type) and contained two 72-bp elements.

Our results suggest the following hypothesis: Since astrocytes are susceptible to both archetypal and nonarchetypal viruses, the most common nonarchetypal SV40 is more often found in brain tumors. Since mesothelial cells are susceptible only or prevalently to nonarchetypal SV40, this less common viral isolate is found in mesotheliomas. In addition, Notch-1 signaling appears to contribute to the susceptibility of astrocytes to archetypal SV40-mediated transformation.

Some of the biological differences between archetypal and nonarchetypal SV40 appear related to the copy number variation of 72-bp elements in the viral regulatory region. Regardless of their position and orientation, the presence of two 72-bp elements exerted a stronger transactivation activity. This finding highlights the enhancer-like nature of the 72-bp sequence and explains why wtSV40-transformed cells contain detectable viral transcripts earlier than 1ESV40-transformed cells.

The 72-bp sequence is also an amplifier of biological effects upon viral infection. Cell transformation requires control of virus replication, suppression of late protein, and enough Tag/tag to overcome cell cycle arrest, apoptosis, and anchorage dependence.<sup>22</sup> Also, the host cell's signaling contributes to this process, in particular, Notch-1, an oncogene that plays a critical role in carcinogenesis, including SV40-mediated carcinogenesis and mesothelioma.<sup>18,26,28</sup>

The early protein Tag binds to the *ori* sequence and initiates virus replication.<sup>2,17</sup> In our transient reporter assays, in the presence of strong transactivation function of Tag, there was no detectable increase of DNA replication. The number of SV40 DNA copies in cells infected by the archetypal and nonarchetypal viruses was comparable. When we evaluated SV40 DNA replication, we observed a spike-shaped curve ([Fig. 3A](#)). Our interpretation supports previous observations<sup>22,23</sup> that cells containing a higher copy number of SV40 particles are lysed, while those carrying low copies survive and can become transformed. This finding is in line with the low copy number of SV40 in clinical samples, which paradoxically led to a debate on the etiological role of SV40 in human cancers.<sup>5,8</sup>

Our reporter assay showed that cellular factors recognized early promoters of either SV40 archetypal and nonarchetypal more strongly than the late promoters (p1 and p2 v. p3 and p4 of [Fig. 4A](#)). As a *trans* element, Tag functions as either an activator or a repressor. Thus, in addition to the reported role of Tag as a repressor of SV40 early transcription,<sup>2,17,29</sup> we verified in our model a strong transactivation activity of Tag on the early promoter by reporter assay in both HM and Ast that led to the accumulation of Tag/tag transcripts. This finding is reminiscent of a previous early report on the regulation of SV40 promoters.<sup>25</sup>

The formation of the Tag/p53 complex inhibits Tag helicase activity.<sup>17</sup> At the same time, the Tag/p53 complex transcriptionally activates IGF-1, stimulating cell growth and contributing to the malignant transformation of HM and astrocytes.<sup>17</sup> Thus, the binding of Tag to p53 contributes to cell transformation at the expense of SV40 replication.

Antisense RNA targeting late protein<sup>23</sup> and microRNA targeting early proteins<sup>29</sup> have both been described in SV40 infections. These reports and our data suggest that when early transcripts outnumber late transcripts, the cell may become transformed; when late transcripts prevail, the cells are lysed (as in permissive monkey CV-1 cells and in human fibroblasts).

A sustained level of Tag expression is critical for transformation; at the same time, host cell proteins play an important role in this process.<sup>30</sup> SV40 activates the hepatocyte growth factor/Met autocrine loop, driving accelerated and invasive cell growth.<sup>19</sup> Notch-1 is transcriptionally induced by wtSV40 early proteins in infected HM.<sup>18</sup> We observed c-Met induction in both HM- and Ast-infected cells in a Tag dose-dependent manner. In Ast/1E and Ast/wt, Notch-1 expression was



induced at higher levels compared to HM. Akt-1 and c-Myc, signaling molecules downstream of c-Met and Notch-1, respectively, are influenced by SV40 infection.<sup>31,32</sup> Accordingly, we found that the activity of Akt-1 (i.e., phospho-Akt) and c-Myc was enhanced by SV40. In infected HM, the increase of Akt-1 activity paralleled that of c-Met expression, while Akt-1 overall protein amount was unchanged, indicating that Akt-1 was under the direct control of c-Met. PTEN did not interfere with Akt-1 activity, as observed in other cell types when Notch-1 is activated and the PI3K/Akt pathway escapes the PTEN control.<sup>33</sup>

Archetypal 1ESV40 induced higher levels of c-Myc compared to nonarchetypal wtSV40. Opposite results were observed in HM. This is an intriguing finding for which we do not have at the current time a convincing explanation. This unexpected, yet reproducible, finding was further confirmed by analyses of the additional downstream Notch-1 targets, Hey-1, Hse-1, and HeyL-1, all of which were induced more efficiently by 1ESV40 compared to wtSV40 (Fig. 5). In future experiments, we will investigate the mechanisms underlying these observed biological differences. These data, however, suggest that Notch-1 induction may also be related to the more frequent association of 1ESV40 with brain tumors compared to wtSV40 that was instead more frequently detected in mesotheliomas.<sup>2,5</sup>

Notch-1 has been related to the process of SV40 transformation of primary HM, and the inhibition of this signaling led to growth arrest of SV40-transformed HM.<sup>26</sup> Notch-1 has also been implicated in Ras-mediated astrocyte transformation.<sup>34</sup> Our results suggest that Notch-1 is required during the early process of SV40-mediated transformation since only cells expressing high levels of Notch-1 were capable of growing in suspension (Figs. 6 and 7).

c-Met activation induces Notch function, which in turn suppresses c-Met.<sup>35</sup> wtSV40 activates c-Met and Notch-1, possibly altering the Met-Notch negative feedback facilitating cellular transformation. Notch-1 is required for phenotype maintenance of glial cells,<sup>36</sup> and overexpression of Notch-1 alone led to rat Schwann cell transformation.<sup>37</sup> Altogether, our results suggest the key role of Notch-1 in promoting survival of the cell in suspension and might provide a clue to the very high susceptibility to SV40-mediated transformation demonstrated by astrocytes (Table 1).

## Materials and Methods

### Cell culture

Human primary mesothelial cells (HM) were derived from pleural or peritoneal effusions of patients pathologically diagnosed free of malignancy in Queen's Medical Center. Human primary astrocytes (Ast) were purchased from Cambrex Bio Science Walkersville Inc. (Chicago, IL) or from Lonza Walkersville Inc. (Walkersville, MD). Monkey kidney fibroblasts CV-1 were purchased from ATCC (Manassas, VA). All cells were maintained in DMEM with 10% fetal bovine serum (FBS) except HM, which were cultured in DMEM containing 20% FBS.

### Viral procedures

776 and Baylor SV40 strains, with different enhancer elements, were used here. The 776/1E was derived from the 776/wt, by partial digestion of plasmid pBRSV2X72, and between the 2 viruses, no other sequences than the regulatory region, including the Tag carboxyl-terminal domain, were modified.<sup>38</sup> Baylor/2E arose from a tissue culture adaptation of the natural archetypal SV40 (Baylor/1E), by duplication of the 72-bp element of the viral regulatory region. In this variant, no modifications were found in the carboxyl-terminal domain of Tag.<sup>39</sup> Viruses were propagated in CV-1 cells, purified by ultracentrifugation on a sucrose layer, and resuspended in DMEM. Virus titer was determined on CV-1 cells, by using Tag immunohistochemistry.<sup>20</sup> Virus infection was carried for 3 hours with occasional shaking, and cells were grown in DMEM with 10% FBS. In this article, 72 hours postinfection is defined as "early infection," and passage numbers are counted from the appearance of "flat foci." Cells were split every 3 days.

The release of virus particles from transformed cells was indirectly estimated by cell viability assay, MTT (Cat no. 11465007001, Roche Diagnostics, Indianapolis, IN) of CV-1 target cells. CV-1 permissive monkey cells were incubated with the conditioned medium of HM, and Ast transformed by the different viruses were collected at passages 4 to 8 after "flat foci" formation. After 96 hours' incubation, MTT assay was used to measure cell viability, as an indicator of cell lysis induced by the presence of viral particles in the conditioned media.

### Real-time PCR

DNA was extracted by using DNeasy Blood & Tissue Kit (Cat no. 69504, Qiagen, Valencia, MD), following conditions recommended by the manufacturer, and amplified using the iCycler iQ system (BioRad, Hercules, CA). In brief, 10 ng of DNA were added to SYBR Green Supermix (Cat no. 170-8882, BioRad). The sequences of the forward and reverse primers were as follows: SV40 (product size: 234 bp), 5'-aactgaggtatt gcttcttc-3' (4924-4907 relative to SV40 776 AF316139) and 5'-aagtaaggtctctcacaag-3' (4680-4710); luciferase pGL4.10 (product size: 168 bp), 5'-cacctctgtgacttccatt-3' and 5'-tgactgaatcgacacaagc-3'; GAPDH (product size: 190 bp), 5'-tggtatctgtgaaggactcatgac-3' and 5'-atgccagt gagctccggttcagc-3'; Hes-1, 5'-tcaacagcacaccggataaa-3' and 5'-ccgcgagctatcttttca-3'; Hey-1, 5'-tggtatcactgaaat gctg-3' and 5'-ttgttgagatgcgaaccag-3'; HeyL-1, 5'-cagtcg gagacgttggaatg-3'. RNA was prepared by the Trizol extraction method (Invitrogen, Carlsbad, CA), followed by DNase I treatment. Primers used for RNA amplification of SV40 early protein Tag (product size: 156 bp) were 5'-ggaactgat gaatgggagcag-3' (4559-4539) and 5'-gaaagtccttggtgttcc tacc-3' (4403-4425). Primers for VP1 mRNA (product size 91 bp) were 5'-cccttagaaagcggtctgtgaa-3' and 5'-tgccatc caccctctg-3'. Each RNA sample was normalized by GAPDH amplification of a 150-bp fragment using primers 5'-gagc cacatgcctcacacac-3' and 5'-catgtagttgaggtcaatgaagg-3'. QuantiTect SYBR Green RT-PCR kit (Cat no. 204243, Qiagen) was used to amplify the RNA template.

### Southern hybridization

Extracted DNA digested with restriction enzymes to completion, loaded onto 1% agarose gel, were transferred to nylon membranes and hybridized with a <sup>32</sup>P-labeled SV40 probe as described.<sup>18</sup>

## Immunological and biochemical assays

Immunohistochemistry was performed on cells grown on chamber slides. Cells were fixed in acetone for 20 minutes and incubated with 1:50 dilution Tag antibody (Cat no. DP01, Calbiochem, San Diego, CA) and processed using the VECTASTAIN ABC kit (Cat no. PK-6102, Vector Laboratories Inc., Burlingame, CA). For immunoblotting, Tag antibody Pab 101 (Santa Cruz Biotechnology Inc., Santa Cruz, CA) was used. Antibodies against Met (C-28) and Notch 1 (C-20)-R were from Santa Cruz Biotechnology Inc. Antibodies against p-Akt /T308 (Cat no. 4056S) and against Akt (Cat no. 9272) were from Cell Signaling (Boston, MA).

## Reporter assay

Different SV40 regulatory regions were subcloned into pGL4.10 firefly luciferase reporter vector (Cat no. E6651, Promega, Madison, WI) and verified by sequencing. Cells (HM and Ast) were seeded at a density of  $3.5 \times 10^4$  cells per well in 48-well dishes, 24 hours prior to transfection. Transient transfection was carried out with a total of 345 ng of DNA that included 45 ng of Renilla luciferase reporter vector pRL-TK (Cat no. E6251, Promega), driven by the CMV promoter as an internal standard, for monitoring transfection efficiency. The promoterless pGL4.10 was used as background control. Cells were exposed to DNA-Lipofectamine (Invitrogen) preparation for 6 hours and then transferred to the appropriate culture media. Expression of reporter gene firefly and Renilla luciferase was measured by standard dual luciferase assay reagents (Promega) 36 and 48 hours posttransfection, when the fluctuation of luciferase activity fell within a 0.5-fold variation. pEarly plasmid expressing Tag and tag under the control of CMV promoter was described previously.<sup>18</sup>

## Cell proliferation

Proliferation curves were obtained by plating  $8 \times 10^4$  cells in triplicate onto 12-well dishes. At 1, 2, 3, and 4 days after plating, cells were counted.

## Anchorage-independence assays

Growth in soft agar: For each T25 flask, a total number of  $10^4$  cells were seeded in 3 mL of 0.3% agar in DMEM containing 10% of fetal bovine serum on top of 0.6% agar in DMEM-FBS in a T25 flask. Agar was allowed to solidify, and cells were incubated for 21 days before counting colonies. Each colony was initially identified when counting 15 cells or more, and final identification was based on progressive growth. Growth on polyHEMA-coated plates: Cell culture plates were coated as described previously,<sup>40</sup> and cells were seeded onto each well of the 96-well plate at densities of 4,000 cells for HM, HM/1E, and HM/wt and 1,500 cells for Ast, Ast/1E, and Ast/wt. Following various periods, 10  $\mu$ L of MTT (Cat no. 11465007001, Roche Diagnostics) was added and further incubated for 3 hours, followed by solubilization overnight. The absorbance was measured at a 595-nm wavelength using a microplate reader. Statistical evaluation was performed by the Student *t* test.

## Notch-1 silencing

For silencing experiments on mesothelial cells, Notch-1 siRNA oligonucleotides from Santa Cruz Biotechnology Inc. (Cat no. sc-36095) were used and transfected according to the manufacturer's protocol. For astrocytes, pshN1-DEST (shN1) expressing a hairpin targeting Notch-1<sup>41</sup> and mock control pDEST(pLenti) were packaged into lentivirus following the manufacturer's recommendation (Cat no. K497500, Invitrogen). Notch-1 knockdown was verified by immunoblotting at day 4 and day 7 posttransduction, respectively.

## Supplementary Material

### Supplementary material

[supp 1 10 1008\\_index.html](#) (840B, html)

## Footnotes

The author(s) declared no potential conflicts of interest with respect to the authorship and/or publication of this article.

The author(s) disclosed receipt of the following financial support for the research and/or authorship of this article: This work was supported by the National Cancer Institute [grant numbers R01 CA92657, R01 CA106567, P01 CA114047 (to M.C.), R01CA134503 (to M.B.), and 5G12 RR003061-24].

Supplementary material for this article is available on the *Genes & Cancer* website at <http://ganc.sagepub.com/supplemental> .

## References

1. Sweet BH, Hilleman MR. The vacuolating virus, S.V. 40. Proc Soc Exp Biol Med. 1960;105:420-7 [DOI] [PubMed] [Google Scholar]

2. Butel JS, Lednický JA. Cell and molecular biology of simian virus 40: implications for human infections and disease. *J Natl Cancer Inst.* 1999;91(2):119-34 [[DOI](#)] [[PubMed](#)] [[Google Scholar](#)]
3. Cutrone R, Lednický J, Dunn G, et al. Some oral poliovirus vaccines were contaminated with infectious SV40 after 1961. *Cancer Res.* 2005;65(22):10273-9 [[DOI](#)] [[PubMed](#)] [[Google Scholar](#)]
4. Cicala C, Pompetti F, Carbone M. SV40 induces mesotheliomas in hamsters. *Am J Pathol.* 1993;142(5):1524-33 [[PMC free article](#)] [[PubMed](#)] [[Google Scholar](#)]
5. Gazdar AF, Butel JS, Carbone M. SV40 and human tumours: myth, association or causality? *Nat Rev Cancer.* 2002;2(12):957-64 [[DOI](#)] [[PubMed](#)] [[Google Scholar](#)]
6. Kean JM, Rao S, Wang M, Garcea RL. Seroepidemiology of human polyomaviruses. *PLoS Pathog.* 2009;5(3):e1000363. [[DOI](#)] [[PMC free article](#)] [[PubMed](#)] [[Google Scholar](#)]
7. Comar M, Rizzardi C, de Zotti R, et al. SV40 multiple tissue infection and asbestos exposure in a hyperendemic area for malignant mesothelioma. *Cancer Res.* 2007;67(18):8456-9 [[DOI](#)] [[PubMed](#)] [[Google Scholar](#)]
8. Carbone M, Albelda SM, Broaddus VC, et al. Eighth international mesothelioma interest group. *Oncogene.* 2007;26(49):6959-67 [[DOI](#)] [[PubMed](#)] [[Google Scholar](#)]
9. Heinsohn S, Szendroi M, Bielack S, Stadt UZ, Kabisch H. Evaluation of SV40 in osteosarcoma and healthy population: a Hungarian-German study. *Oncol Rep.* 2009;21(2):289-97 [[PubMed](#)] [[Google Scholar](#)]
10. Shivapurkar N, Harada K, Reddy J, et al. Presence of simian virus 40 DNA sequences in human lymphomas. *Lancet.* 2002;359(9309):851-2 [[DOI](#)] [[PubMed](#)] [[Google Scholar](#)]
11. Vilchez RA, Madden CR, Kozinetz CA, et al. Association between simian virus 40 and non-Hodgkin lymphoma. *Lancet.* 2002;359(9309):817-23 [[DOI](#)] [[PubMed](#)] [[Google Scholar](#)]
12. Capello D, Rossi D, Gaudino G, Carbone A, Gaidano G. Simian virus 40 infection in lymphoproliferative disorders. *Lancet.* 2003;361(9351):88-9 [[DOI](#)] [[PubMed](#)] [[Google Scholar](#)]
13. Malkin D, Chilton-MacNeill S, Meister LA, Sexsmith E, Diller L, Garcea RL. Tissue-specific expression of SV40 in tumors associated with the Li-Fraumeni syndrome. *Oncogene.* 2001;20(33):4441-9 [[DOI](#)] [[PubMed](#)] [[Google Scholar](#)]
14. Mendoza SM, Konishi T, Miller CW. Integration of SV40 in human osteosarcoma DNA. *Oncogene.* 1998;17(19):2457-62 [[DOI](#)] [[PubMed](#)] [[Google Scholar](#)]
15. Yamamoto H, Nakayama T, Murakami H, et al. High incidence of SV40-like sequences detection in tumour and peripheral blood cells of Japanese osteosarcoma patients. *Br J Cancer.* 2000;82(10):1677-81 [[DOI](#)] [[PMC free article](#)] [[PubMed](#)] [[Google Scholar](#)]
16. Carbone M, Rizzo P, Grimley PM, et al. Simian virus-40 large-T antigen binds p53 in human mesotheliomas. *Nat Med.* 1997;3(8):908-12 [[DOI](#)] [[PubMed](#)] [[Google Scholar](#)]
17. Bocchetta M, Elias S, De Marco MA, Rudzinski J, Zhang L, Carbone M. The SV40 large T antigen-p53 complexes bind and activate the insulin-like growth factor-I promoter stimulating cell growth. *Cancer Res.* 2008;68(4):1022-9 [[DOI](#)] [[PubMed](#)] [[Google Scholar](#)]
18. Bocchetta M, Miele L, Pass HI, Carbone M. Notch-1 induction, a novel activity of SV40 required for growth of SV40-transformed human mesothelial cells. *Oncogene.* 2003;22(1):81-9 [[DOI](#)] [[PubMed](#)] [[Google Scholar](#)]
19. Cacciotti P, Libener R, Betta P, et al. SV40 replication in human mesothelial cells induces HGF/Met receptor activation: a model for viral-related carcinogenesis of human malignant mesothelioma. *Proc Natl Acad Sci U S A.* 2001;98(21):12032-7 [[DOI](#)] [[PMC free article](#)] [[PubMed](#)] [[Google Scholar](#)]
20. D'Alisa RM, Gershey EL. On the quantitation of SV40 virus by plaque assay and immunoperoxidase technique. *J Histochem Cytochem.* 1978;26(9):755-8 [[DOI](#)] [[PubMed](#)] [[Google Scholar](#)]
21. Carbone M, Klein G, Gruber J, Wong M. Modern criteria to establish human cancer etiology. *Cancer Res.* 2004;64(15):5518-24 [[DOI](#)] [[PubMed](#)] [[Google Scholar](#)]
22. Fahrbach KM, Katzman RB, Rundell K. Role of SV40 ST antigen in the persistent infection of mesothelial cells. *Virology.* 2008;370(2):255-63 [[DOI](#)] [[PMC free article](#)] [[PubMed](#)] [[Google Scholar](#)]
23. Carbone M, Pannuti A, Zhang L, Testa JR, Bocchetta M. A novel mechanism of late gene silencing drives SV40 transformation of human mesothelial cells. *Cancer Res.* 2008;68(22):9488-96 [[DOI](#)] [[PMC free article](#)] [[PubMed](#)] [[Google Scholar](#)]
24. Testa JR, Giordano A. SV40 and cell cycle perturbations in malignant mesothelioma. *Semin Cancer Biol.* 2001;11(1):31-8 [[DOI](#)] [[PubMed](#)] [[Google Scholar](#)]

25. Das GC, Niyogi SK, Salzman NP. SV40 promoters and their regulation. *Prog Nucleic Acid Res Mol Biol*. 1985;32:217-36 [DOI] [PubMed] [Google Scholar]
26. Graziani I, Elias S, De Marco MA, et al. Opposite effects of Notch-1 and Notch-2 on mesothelioma cell survival under hypoxia are exerted through the Akt pathway. *Cancer Res*. 2008;68(23):9678-85 [DOI] [PubMed] [Google Scholar]
27. Sangar D, Pipkin PA, Wood DJ, Minor PD. Examination of poliovirus vaccine preparations for SV40 sequences. *Biologicals*. 1999;27(1):1-10 [DOI] [PubMed] [Google Scholar]
28. Rizzo P, Osipo C, Foreman K, Golde T, Osborne B, Miele L. Rational targeting of Notch signaling in cancer. *Oncogene*. 2008;27(38):5124-31 [DOI] [PubMed] [Google Scholar]
29. Sullivan CS, Grundhoff AT, Tevethia S, Pipas JM, Ganem D. SV40-encoded microRNAs regulate viral gene expression and reduce susceptibility to cytotoxic T cells. *Nature*. 2005;435(7042):682-6 [DOI] [PubMed] [Google Scholar]
30. Pagano JS, Blaser M, Buendia MA, et al. Infectious agents and cancer: criteria for a causal relation. *Semin Cancer Biol*. 2004;14(6):453-71 [DOI] [PubMed] [Google Scholar]
31. Morike M, Quaiser A, Muller D, Montenarh M. Early gene expression and cellular DNA synthesis after stimulation of quiescent NIH3T3 cells with serum or purified simian virus 40. *Oncogene*. 1988;3(2):151-8 [PubMed] [Google Scholar]
32. Cacciotti P, Barbone D, Porta C, et al. SV40-dependent AKT activity drives mesothelial cell transformation after asbestos exposure. *Cancer Res*. 2005;65(12):5256-62 [DOI] [PubMed] [Google Scholar]
33. Gutierrez A, Look AT. NOTCH and PI3K-AKT pathways intertwined. *Cancer Cell*. 2007;12(5):411-3 [DOI] [PubMed] [Google Scholar]
34. Kanamori M, Kawaguchi T, Nigro JM, et al. Contribution of Notch signaling activation to human glioblastoma multiforme. *J Neurosurg*. 2007;106(3):417-27 [DOI] [PubMed] [Google Scholar]
35. Stella MC, Trusolino L, Pennacchiotti S, Comoglio PM. Negative feedback regulation of Met-dependent invasive growth by Notch. *Mol Cell Biol*. 2005;25(10):3982-96 [DOI] [PMC free article] [PubMed] [Google Scholar]
36. Li H, Chang YW, Mohan K, et al. Activated Notch1 maintains the phenotype of radial glial cells and promotes their adhesion to laminin by upregulating nidogen. *Glia*. 2008;56(6):646-58 [DOI] [PMC free article] [PubMed] [Google Scholar]
37. Li Y, Rao PK, Wen R, et al. Notch and Schwann cell transformation. *Oncogene*. 2004;23(5):1146-52 [DOI] [PubMed] [Google Scholar]
38. Lednický JA, Wong C, Butel JS. Artificial modification of the viral regulatory region improves tissue culture growth of SV40 strain 776. *Virus Res*. 1995;35(2):143-53 [DOI] [PubMed] [Google Scholar]
39. Lednický JA, Butel JS. Tissue culture adaptation of natural isolates of simian virus 40: changes occur in viral regulatory region but not in carboxy-terminal domain of large T-antigen. *J Gen Virol*. 1997;78(Pt 7):1697-705 [DOI] [PubMed] [Google Scholar]
40. Fukazawa H, Mizuno S, Uehara Y. A microplate assay for quantitation of anchorage-independent growth of transformed cells. *Anal Biochem*. 1995;228(1):83-90 [DOI] [PubMed] [Google Scholar]
41. Chen Y, De Marco MA, Graziani I, et al. Oxygen concentration determines the biological effects of NOTCH-1 signaling in adenocarcinoma of the lung. *Cancer Res*. 2007;67(17):7954-9 [DOI] [PubMed] [Google Scholar]

## Associated Data

---

*This section collects any data citations, data availability statements, or supplementary materials included in this article.*

## Supplementary Materials

### Supplementary material

[supp\\_1\\_10\\_1008\\_index.html](#) (840B, html)

[supp\\_1947601910395580\\_DS\\_10.1177\\_1947601910395580\\_FigS1.pdf](#) (143.1KB, pdf)

[supp\\_1947601910395580\\_DS\\_10.1177\\_1947601910395580\\_FigS2.pdf](#) (106.7KB, pdf)

